Environmental Science
Water Research & Technology

ROYAL SOCIETY OF CHEMISTRY

PAPER

View Article Online
View Journal | View Issue

Cite this: *Environ. Sci.: Water Res. Technol.*, 2025, **11**, 1898

Elimination of miconazole nitrate from water by electro-Fenton: effect of operating parameters and degradation pathway†

Nadia Gadi,[ab] Allisson Barros de Souza,[ce] Nadine C. Boelee,[a] Deirdre Cabooter [e] and Raf Dewil [*bd]

This study investigates the removal of miconazole, a widely used pharmaceutical, from water using the electro-Fenton process. By systematically evaluating key parameters such as applied current intensity (10–500 mA), catalyst concentration (0.1–1.0 mM Fe^{2+}), and water matrix composition, optimal conditions for maximizing pollutant removal efficiency were identified. The highest first-order oxidation rate constant of 36.4×10^{-2} min^{-1} was achieved under optimal conditions, demonstrating the efficiency of the electro-Fenton process. Total organic carbon (TOC) removal reached a maximum of 90% after 180 min of treatment, indicating significant mineralization of the pollutant. Ten major aromatic oxidation intermediates were identified using ultra-high-performance liquid chromatography coupled with high-resolution mass spectrometry (UHPLC-HRMS), providing valuable insight into the degradation pathways. This study stands out for its comprehensive optimization of key parameters, ensuring robust and practical application of the electro-Fenton process for pharmaceutical removal. Achieving 90% TOC removal and a high oxidation rate constant (36.4×10^{-2} min^{-1}) demonstrates superior mineralization efficiency. The identification of ten major degradation intermediates *via* UHPLC-HRMS provides valuable insight into pollutant breakdown pathways. Additionally, by considering real water matrix effects, this work enhances the practical applicability of electro-Fenton in sustainable wastewater treatment. The obtained results highlight the electro-Fenton process as an effective and promising technology for the removal and mineralization of pharmaceutical contaminants from water, contributing to the advancement of sustainable wastewater treatment solutions.

Received 15th June 2024,
Accepted 2nd May 2025

DOI: 10.1039/d4ew00508b

rsc.li/es-water

Water impact

Electro-Fenton degradation of miconazole nitrate achieves 90% pollutant removal, offering a powerful solution for pharmaceutical micropollutants in water. This study identifies key degradation intermediates and optimal treatment conditions, advancing electrochemical methods as sustainable alternatives for improved wastewater treatment and public health protection.

1. Introduction

Over the last decade, micropollutants (MPs) have received considerable attention, especially pharmaceuticals and personal care products (PPCPs), since the latter are the most widely detected compounds in municipal wastewater.[1,2] Most of the pharmaceuticals detected in wastewater emerge from domestic use, and a study on the disposal habits of the American population indicated that only 1.4% of people returned unused drugs to drug stores, but 54% threw them away and 35.4% disposed of them in the sink or toilet.[3] Unfortunately, the effects of these compounds, metabolites, and transformation products on human health and the ecosystem remain unclear.[4]

Miconazole (MCZ) is of interest since it is not completely removed by conventional treatment methods, and it is detected at an average concentration of 6–26 ng L^{-1} in wastewater treatment plant effluents.[5] Furthermore, MCZ is

[a] *Nijhuis Industries, PO Box 44, 7000 AA Doetinchem, The Netherlands*
[b] *KU Leuven, Department of Chemical Engineering, Process and Environmental Technology Lab, Sint-Katelijne-Waver, Belgium. E-mail: raf.dewil@kuleuven.be*
[c] *Agilent Technologies Deutschland, Hewlett-Packard-Strasse 8, 76337 Waldbronn, Germany*
[d] *University of Oxford, Department of Engineering Science, Oxford, UK*
[e] *KU Leuven, Department of Pharmaceutical and Pharmacological Sciences, Pharmaceutical Analysis, Herestraat 49, 3000 Leuven, Belgium*
† Electronic supplementary information (ESI) available. See DOI: https://doi.org/10.1039/d4ew00508b

included in the surface water watch list adopted by the European Commission.[6] MCZ is a weak base poorly soluble in water; it belongs to the azole group of antifungals, which is known as the largest class of antimycotic drugs in clinical use,[7] and it is often used to treat skin infections.[8]

In this work, electro-Fenton (EF) technology is used to treat water containing MCZ. The EF process is an electrochemical advanced oxidation process (eAOP), which has attracted much attention because of its capability to remove a wide range of contaminants of emerging concern and organic pollutants.[9,10] EF is an environmentally compatible technique since it uses *in situ*-generated clean reagents such as hydroxyl radicals (HO·) to degrade pollutants, thus avoiding the use of harmful chemical reagents.[10,11] During the EF process, HO· is produced (i) through the Fenton reaction (eqn (1)) for indirect oxidation and (ii) at the anode surface for direct oxidation of organics when a material with a high oxygen evolution potential, such as boron-doped diamond (BDD), is used. BDD is known to be the most powerful electrode for oxidation in eAOPs (eqn (2)).[10,12] HO· is a nonselective species that oxidizes organics and organometallic substances that are present in water[13] and is considered one of the most powerful oxidants, with a standard redox potential $E^{\circ}(\cdot OH/H_2O)$ = 2.80 V/SHE.[9,13]

$$Fe^{2+} + H_2O_2 \rightarrow Fe^{3+} + HO\cdot + HO^- \quad (1)$$

$$BDD + H_2O \rightarrow BDD(HO)\cdot + H^+ + e^- \quad (2)$$

$$Fe^{3+} + e^- \rightarrow Fe^{2+} \quad (3)$$

$$O_2 + 2H^+ + 2e^- \rightarrow H_2O_2 \quad (4)$$

Another advantage of EF resides in its ability to electrochemically generate Fenton's reagents *in situ*. Hydrogen peroxide H_2O_2 is produced *via* a two electron ($2e^-$) oxygen reduction reaction when a carbonaceous material such as carbon felt (CF) or carbon sponge is used as a cathode (eqn (4)), while Fe^{2+} is regenerated by the $1e^-$ reduction of Fe^{3+} (eqn (3)).[14] This avoids the use of large quantities of reagents and costs related to H_2O_2 purchase and transport as well as the risks associated with its storage.[15] The catalyst regeneration during the EF process plays a crucial role in the process effectiveness as it directly relates to the amount of HO· formed which is central to the oxidation process.[16] Several studies have focused on the improvement of the Fe^{2+} regeneration using different methods such as (i) pulsed current instead of continuous current which allows a better control of the timing of the ion exchange reaction, (ii) electron transfer control using a single-atom catalyst to maximize the availability of active sites where electron transfer can occur, and (iii) magnetic field application near the electrode to improve fluid dynamics and overall mass transfer near the electrode surface.[16] These approaches collectively increase process efficiency and reduce reaction time, which are crucial parameters for process scaling up.

This study explores the removal of miconazole, a widely used yet under-studied pharmaceutical, from wastewater using the EF process with a BDD anode and CF cathode. By determining the optimal operating conditions: current density, pH, and catalyst concentration based on degradation kinetics and removal efficiencies, the research provides valuable insights into effective treatment strategies. Additionally, the study identifies and analyzes degradation by-products through UHPLC-QTOF MS, often overlooked in similar studies, proposing a degradation pathway and highlighting the importance of addressing both the parent compound and its potentially toxic intermediates for comprehensive environmental remediation.

2. Materials and methods

2.1 Reagents

All chemicals were used as received without further purification. Miconazole nitrate ($C_{18}H_{14}Cl_4N_2O\cdot HNO_3$, purity >97.5%) was supplied by Fisher Scientific (Landsmeer, The Netherlands). Iron sulfate heptahydrate ($FeSO_4{\cdot}7H_2O$, 99%) was acquired from Acros Organics (Geel, Belgium), and sodium sulfate (Na_2SO_4) was acquired from Boom Chemicals (Meppel, The Netherlands). Sulfuric acid (H_2SO_4, 96%), acetonitrile (CH_3CN, 99.9%), and phosphoric acid (H_3PO_4, 85%) were obtained from Sigma-Aldrich (Schnelldorf, Germany), while Milli-Q water was obtained in the lab using a Milli-Q water purification system from Merck (Millipore, USA).

2.2 Experimental procedure

To ensure complete dissolution, MCZ was dissolved in ultrapure water (Milli-Q), the pH of which was adjusted to 3.0 using H_2SO_4, and subsequently heated to 50 °C for 30 min. After turning off the heating, the mixture was stirred overnight (≥14 h).

The EF experiments were carried out in an undivided cylindrical glass electrochemical cell of 700 mL with a two-electrode system placed in the center of the cell with a gap of 1 cm. The electrodes were soft graphite felt (10 cm × 6 cm × 0.4 cm) supplied by Mersen BV Benelux used as a cathode, together with a boron-doped diamond mesh (BDD) anode (10 cm × 5 cm × 0.1 cm) obtained from Neocoat® (La Chaux-de-Fonds, Switzerland). The electrochemical cell was filled with a 500 ml solution of miconazole nitrate at a concentration of 50 mg L^{-1} (0.11 mM), 0.2 mM of Fe^{2+}, and 50 mM of Na_2SO_4 as a catalyst and supporting electrolyte. The pH was adjusted to 3.0 using H_2SO_4. In addition to homogenizing the solution, the air bubbling ensured during the EF treatment provided oxygen for the generation of H_2O_2 by a $2e^-$ oxygen reduction at the cathode. During the experiments, aliquots were collected from the beaker for analysis of MCZ and TOC concentrations. The data presented in this study represent the average values from duplicate experiments.

2.3 Analytical methods

2.3.1 Miconazole and metal concentrations. The MCZ concentration in the samples was analyzed using high-performance liquid chromatography with diode array detection. An Agilent 1260 Infinity II Prime LC system (Agilent Technologies, Waldbronn, Germany), consisting of a binary pump, a multisampler, a column compartment, and a diode array detector, was used. A reversed-phase column (Zorbax RRHD SB-Aq 2.1 × 50 mm; d_p 1.8 μm, Agilent Technologies) equipped with a guard column (Zorbax RRHD SB-Aq 2.1 × 5 mm; d_p 1.8 μm, Agilent Technologies) was used. The mobile phase consisted of water (A) and acetonitrile (B), both acidified with 0.1% orthophosphoric acid, which were employed for the chromatographic separations. Gradient elution was applied, increasing from 25% to 95% B in 5 min, held for 1 min at 95% B, returned to initial conditions (25% B) in 0.1 min, and maintained for 2 min for column re-equilibration. The mobile phase flow rate was 0.45 mL min^{-1}, the injection volume was 1 μL, and the column compartment was kept at 40 °C. DAD detection was performed at a wavelength of 220 nm.

The removal% of MCZ throughout the EF treatment was calculated using the following equation (eqn (5))

$$\text{MCZ removal\%} = \frac{\text{MCZ}_0 - \text{MCZ}_t}{\text{MCZ}_0} \times 100 \quad (5)$$

where MCZ_0 is the concentration of MCZ before treatment and MCZ_t is the value at time t. Both values are expressed in mg L^{-1}.

The concentration of heavy metals (Fe, Mn, Zn, Cu) in the WWE was detected by inductively coupled plasma mass spectrometry (ICP-MS, Optima 8300) at a temperature of 25 °C following the NEN-EN-ISO 17294-2(2004) method.

2.3.2 Transformation product identification. For the identification of the transformation products, a UHPLC-QTOF-MS system was used. An Agilent 1290 Infinity II UHPLC system consisting of a binary pump, a vial sampler, a column compartment, and a diode array detector was used in combination with an Agilent 6550 iFunnel quadrupole time-of-flight mass spectrometer (QTOF-MS) operated in the 2 GHz extended dynamic range mode (both from Agilent Technologies). Chromatographic separations were performed on a Zorbax RRHD SB-Aq column (2.1 × 100 mm; d_p 1.8 μm, Agilent Technologies) equipped with a guard column (Zorbax RRHD SB-Aq 2.1 × 5 mm; d_p 1.8 μm, Agilent Technologies). The mobile phase consisted of water (A) and acetonitrile (B), both acidified with 0.1% formic acid. Gradient elution was applied, increasing from 5 to 95% B in 7 min; 95% B was held for 1 min and returned to initial conditions (5% B) in 0.1 min; 5% B was held for 2 min for column re-equilibration. The mobile phase flow rate was 0.45 mL min^{-1}, the column compartment was kept at 40 °C, the injection volume was 5 μL, and DAD detection was set at 220 nm. The ionization was performed in positive electrospray ionization mode using Dual Agilent Jet Stream Technology operated at a gas temperature of 2250 °C, drying gas flow of 15 L min^{-1}, nebulizer pressure of 35 psi, and a sheath gas temperature and flow of 350 °C and 12 L min^{-1}, respectively. The capillary voltage was set at 4000 V, nozzle voltage at 500 V, and fragmentor at 350 V. MS and MS/MS spectra were collected at 3 spectra s^{-1}. Data analysis was performed on Agilent MassHunter Qualitative (version 10.0), and molecular features were extracted on Agilent MassHunter Profinder (version 10.0.2) software.

2.3.3 Total organic carbon analysis. Mineralization of MCZ was monitored by total organic carbon (TOC) removal, measured by a Shimadzu TOC analyzer (TOC-LCSH/CSN Standalone, 's-Hertogenbosch, Netherlands). TOC removal was calculated using the following equation (eqn (6)):

$$\text{TOC removal\%} = \frac{\text{TOC}_0 - \text{TOC}_t}{\text{TOC}_0} \times 100 \quad (6)$$

where TOC_0 is the value before treatment and TOC_t is the value at time t. Both values are expressed in mg L^{-1}. These data were used to calculate the mineralization current efficiency MCE (eqn (7)):

$$\text{MCE}\ (\%) = \frac{nFV(\text{TOC}_0 - \text{TOC}_t)}{4.32 \times 10^7\ mIt} \quad (7)$$

where n represents the number of electrons consumed per MCZ molecule during mineralization, which was 66 according to the mineralization reaction given in eqn (9), F is the Faraday constant (96.485 C mol^{-1}), 4.32×10^7 represents the conversion factor used to homogenize the units (3600 s h^{-1} × 12 000 mg C mol^{-1}), m is the number of MCZ carbon atoms,[17] and I and t are the current intensity and time, respectively. TOC_0 is the value before treatment, and TOC_t is the value at time t.

Since the process was completed at a constant current (I), the energy consumption per unit of TOC mass (EC_{TOC}) was calculated using (eqn (8)):

$$\text{EC}_{\text{TOC}}\left(\text{kW h per g}_{\text{TOC}}\right) = \frac{E_{\text{cell}} It}{\Delta(\text{TOC})_{\text{exp}} V} \quad (8)$$

where E_{cell} is the average potential difference of the cell (V), I the applied current intensity (A), V the volume of the treated solution in (L), t the electrolysis time (h), and $\Delta(TOC)_{exp}$ the experimental TOC decay (g L^{-1}).

$$C_{18}H_{15}Cl_4NO_4 + 32H_2O \rightarrow 18CO_2 + 67H^+ + 3NH_4^+ + 4Cl^- + 66e^- \quad (9)$$

3. Results and discussion

The most important parameters affecting the EF process are the pH value, current intensity, and concentration of the catalyst.[18] In this study, the pH was fixed at 3.0, as it was previously proven that this value was optimal for Fenton's reaction due to the solubility of Fe^{2+}.[17,19,20] The effect of the water matrix was investigated by comparing degradation and

mineralization rates in PW and WWE, as well as the effect of the initial concentration of the targeted compound.

3.1 Effect of the initial concentration of MCZ

The results in Fig. 1 highlight how the initial concentration of miconazole (MCZ) affects both the degradation rate and removal efficiency during electro-Fenton (EF) treatment. Experiments were carried out under consistent conditions of 0.25 A current, 50 mM Na_2SO_4 as electrolyte, 0.15 mM Fe^{2+} as the catalyst, and pH 3.0, while the MCZ concentration varied from 10 mg L^{-1} to 100 mg L^{-1}.

At the lowest MCZ concentration of 10 mg L^{-1}, rapid removal was achieved within less than 2 minutes (Fig. 1a), making it challenging to evaluate the degradation kinetics precisely due to the short reaction time. As the initial concentration of MCZ was increased to 50 mg L^{-1} and 100 mg L^{-1}, complete removal was still achieved but required approximately 30 minutes. The observed removal rate constants were 0.186 min^{-1} for 50 mg L^{-1} and a slightly higher 0.203 min^{-1} for 100 mg L^{-1} (Table 1), suggesting that as the pollutant concentration rises, so does the rate of degradation, potentially due to the increased availability of target molecules for hydroxyl radical (HO·) attack. However, at higher MCZ concentrations, HO· becomes a limiting factor, as more organic molecules compete for the same quantity of radicals.[21]

The mineralization efficiency (Fig. 1b) showed an inverse relationship with MCZ concentration: higher concentrations resulted in lower mineralization rates. For example, in the first 30 minutes of treatment, mineralization efficiencies reached 60%, 57%, and 45% for MCZ concentrations of 100 mg L^{-1}, 50 mg L^{-1}, and 10 mg L^{-1}, respectively. This inverse trend can be attributed to the buildup of organic intermediates near the electrode at higher MCZ concentrations, accelerating the initial degradation but limiting the overall mineralization efficiency.[22] Higher concentrations of organics require more HO· radicals per unit of pollutant, which makes HO·, when unavailable in sufficient quantity, the limiting reagent restricting mineralization.[23] This consequently leads to an accumulation of organic compounds during the treatment and lower removal rates.[22,24]

After the initial 30 minutes, mineralization slowed, with only an additional 7% to 13% achieved in the subsequent 30 minutes. By this stage, most easily degradable organics had been removed, and the remaining concentration was low, making mass transfer limitations more significant.[25] Under these constant experimental conditions, the formation rate of HO· and M(HO·) remained constant. As the organic matter concentration decreased over time, the HO· to pollutant ratio increased, leading to surplus HO· that could undergo side reactions, further reducing the mineralization efficiency through parasitic losses (eqn (10)).[26]

$$2HO\cdot \rightarrow H_2O_2 \quad (10)$$

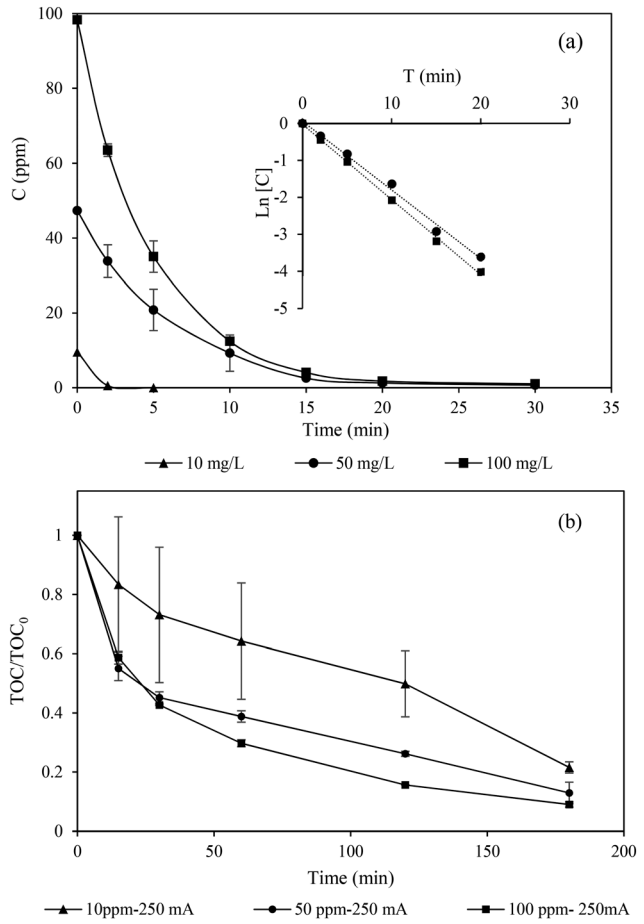

Fig. 1 Effect of the initial concentration of MCZ on its degradation (a) and mineralization (b) during electro-Fenton treatment at a constant current intensity of 200 mA, [Na_2SO_4] = 50 mM, Fe^{2+} = 0.2 mM and pH = 3.0.

3.2 Effect of applied current

The current intensity is a crucial EF parameter because it is directly related to the energy consumption and costs of the process, and governs the production of HO· and H_2O_2 as well as the electrochemical regeneration of Fe^{2+} (eqn (3)). The removal of MCZ at a current intensity ranging from 50 mA to 500 mA was studied. It was observed that the MCZ concentration starts decreasing as soon as the current is applied (Fig. 2a) to achieve total removal after 15 min, 20 min, 30 min, and 60 min when 500 mA, 150 mA, 250 mA, and 50 mA are applied, respectively. The first-order reaction constants are shown in Table 1. The highest removal rate was observed at the highest applied current intensity of 500 mA. This is because a large amount of HO· and BDD(HO·) are produced in the bulk (eqn (1)) and at the anode surface (eqn (2)) when a high current intensity is applied.[19,27] However, side reactions such as the production of oxygen at the anode (eqn (10)) and the evolution of hydrogen (eqn (11)) at the cathode[19] might also have been triggered at this current intensity, since the removal rate observed at 150 mA (0.31 min^{-1}) was very close to that

Table 1 First-order (k_1) and second-order (k_2) reaction rate constants for degradation and mineralization of MCZ, respectively, under different experimental conditions

Fixed parameters	pH = 3.0 $[MCZ]_0$ = 50 mM Fe^{2+} = 0.2 mM				
Variable parameter	I (mA)	50	150	250	500
	k_1 (min^{-1})	0.070	0.310	0.186	0.344
	R^2	0.964	0.975	0.993	0.991
	$k_2 \times 10^{-3}$ (mg^{-1} min^{-1})	0.40	2.30	1.30	1.90
	R^2	0.985	0.985	0.972	0.975
Fixed parameters	pH = 3.0 I = 150 mA Fe^{2+} = 0.2 mM				
Variable parameter	$[MCZ]_0$ (mg L^{-1})	10	50	100	
	k_1 (min^{-1})	nd	0.186	0.203	
	R^2	—	0.993	0.999	
	$k_2 \times 10^{-3}$ (mg^{-1} min^{-1})	2.4	1.3	0.8	
	R^2	0.981	0.993	0.994	
Fixed parameters	pH = 3.0 I = 150 mA $[MCZ]_0$ = 50 mg L^{-1}				
Variable parameter	$[Fe^{2+}]$ (mM)	0	0.1	0.2	0.3
	k_1 (min^{-1})	0.148	0.263	0.186	0.236
	R^2	0.996	0.984	0993	0.978
	$k_2 \times 10^{-3}$ (mg^{-1} min^{-1})	2.5	1.1	1.2	1.1
	R^2	0.983	0.922	0.993	0.989
Fixed parameters	pH = 3.0 $[MCZ]_0$ = 50 mg L^{-1} I = 150 mM Fe^{2+} = 0.2 mM matrix: WWE				
	k_1 (min^{-1})	0.364			
	R^2	0.995			
	$k_2 \times 10^{-3}$ (mg^{-1} min^{-1})	0.8			
	R^2			0.931	

observed at 500 mA (0.34 min^{-1}). Moreover, the increase in the applied current from 50 mA to 150 mA led to an approximate 3-fold increase in the degradation rate constant and an approximate 5-fold increase in mineralization. However, the increase in current from 150 mA to 500 mA led to a slight increase in the removal rate constant (0.31 min^{-1} to 0.3 min^{-1}). A lower removal rate was observed at 250 mA compared to 150 mA. The reduced efficiency at the intermediate current of 250 mA can be attributed to a combination of radical recombination into less reactive species like H_2O_2 (eqn (10)) or O_2, reducing their availability for pollutant degradation. Simultaneously, the potential at the electrode surface may promote OER, consuming electrons that would otherwise generate reactive oxygen species.[28] Additionally, less optimal mass transfer at 250 mA can limit the interaction between radicals and pollutants, while byproducts accumulating near the electrode can hinder further reactions.[24] These results emphasize the importance of optimizing current density to minimize side reactions and enhance the process efficiency.[22]

The mineralization kinetics and efficiencies are in accordance with the removal of MCZ for the reasons stated above. The mineralization follows a similar evolution, with the fastest mineralization during the first 30 min where approximately 50% to 60% of the organics are mineralized. After 30 min, slower rates are observed in all the experiments suggesting that the compounds formed during the successive attacks of radicals on MCZ are more recalcitrant to the action of the EF process.[29] Considering these results, the optimal current intensity for MCZ degradation would be 150 mA, which provided 100% MCZ removal after 20 min of treatment and 85% mineralization after a reaction time of 20 min with an energy consumption ranging between 0.05 and 0.2 KW h per g_{TOC}.

$$2H_2O \rightarrow 4H^+ + O_2 + 4e^- \quad (11)$$

3.2.a Energy consumption and mineralization current efficiency. The observed decrease in MCE (Fig. 3) and decrease in EC (Fig. 4) in this study are in good agreement with the observed mineralization rates (Fig. 2b and Table 1). The MCE values decrease while the energy consumption per unit of TOC removed increases as the current applied to the system increases. An MCE value of 79% was obtained at 15 min for I = 150 mA; for most of the applied currents, the highest MCE was observed at the early stage of electrolysis, indicating fast mineralization of MCZ into CO_2. The decrease in MCE% can be explained by the reduction in the concentration of organic matter in the solution leading to a decrease in the rate of mineralization on the one hand and the enhancement of the parasitic reactions on the other hand. The formation of intermediates that are more difficult to mineralize constitutes another explanation.[27,30] Greater MCE and lower EC are obtained compared to those reported in the literature.[31] An MCE varying between 25%

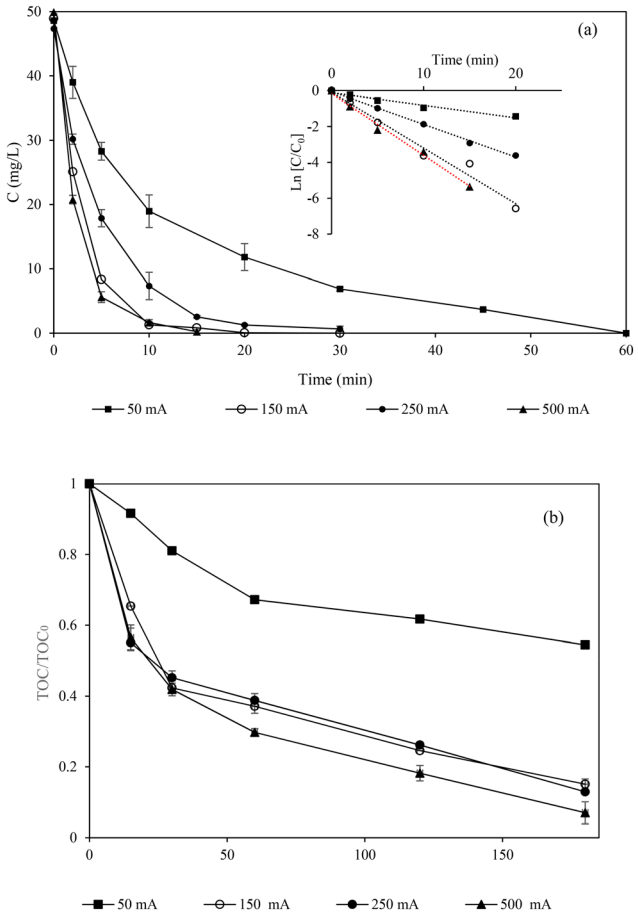

Fig. 2 Effect of the applied current intensity on miconazole degradation (a) and mineralization (b) during electro-Fenton treatment [Na_2SO_4] = 50 mM, Fe^{2+} = 0.2 mM and pH = 3.0.

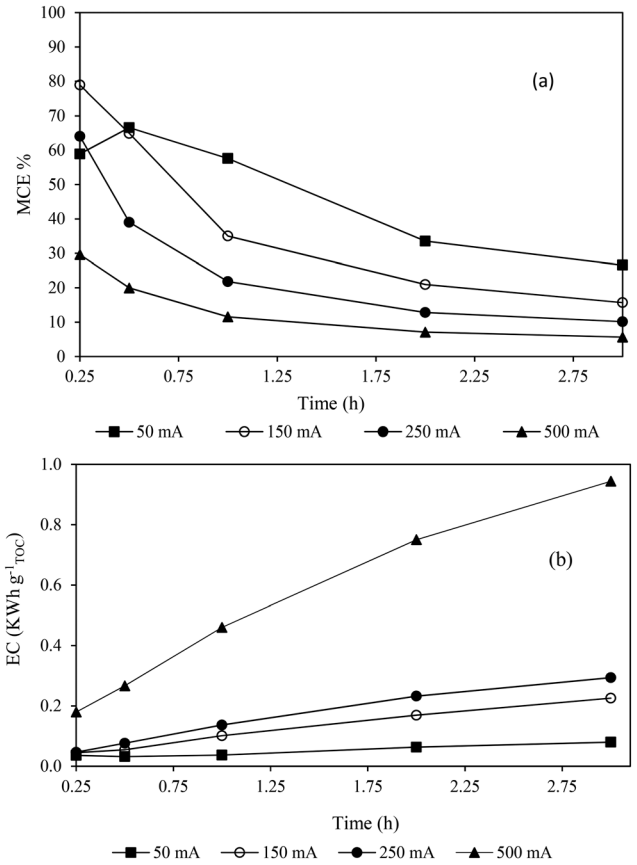

Fig. 3 Mineralization current efficiency (% MCE) (a) and energy consumption (EC_{TOC}) (b) as a function of electrolysis time of 50 mg L^{-1} of miconazole corresponding to 25.95 mg L^{-1} initial TOC by electro-Fenton under operating conditions of [Na_2SO_4] = 50 mM, Fe^{2+} = 0.2 mM and pH = 3.0.

and 10% was obtained, and EC values increased from 0.2 to 0.3 kW h per g_{TOC} during a 3 h treatment of a 250 mL solution of amoxicillin at a concentration of 0.1 mM and current of 120 mA, indicating a more efficient use of energy in the current study.

3.3 Effect of catalyst (Fe^{2+}) concentration

Fe^{2+} ions play an important role in initiating the decomposition of H_2O_2 to form OH·. A concentration of 0.1 to 0.2 mM Fe^{2+} is usually employed when CF is used as a cathode.[27] In this work, a set of experiments with concentrations ranging from 0 mM (anodic oxidation (AO)) to 0.3 mM were performed to find the optimal concentration for MCZ removal. As shown in Fig. 4a and Table 1, slower degradation rates are obtained during the AO process than during the EF process. During AO, only heterogeneous M(HO·) can be formed due to the absence of Fe^{2+}. Hence, the amount of oxidants formed in the bulk is higher during EF,[27] which explains the difference in the removal rates. These results clarify the contributions of direct and indirect oxidation to MCZ removal, quantified through kinetic rate constants (Table 1). Anodic oxidation alone yielded a rate constant of 0.186 min^{-1}, while combining Fenton's reaction with anodic oxidation increased the rate constant to 0.263 min^{-1}. This enhancement of 70% reflects the additional oxidative contribution from the Fenton reaction, emphasizing the complementary role of hydroxyl radicals generated through Fenton chemistry in achieving more efficient MCZ degradation. Furthermore, it was observed that the decay in MCZ concentration was very similar when the Fe^{2+} concentration was increased from 0.1 mM to 0.3 mM (Fig. 3a). Normally, the Fe^{2+} concentration has a strong effect on the removal of compounds since it is directly related to the amount of HO· formed *via* the Fenton reaction (eqn (1)).[32] The observed behavior indicates that the Fenton reaction might be limited by other parameters, such as H_2O_2 generation (eqn (4)). In contrast, the TOC decrease (Fig. 4b and Table 1) was twice as high when no iron was added to the medium (AO). This is an unusual behavior because EF is usually much more powerful than AO for aromatic pollutant degradation under the present experimental conditions.[12] This could be a result of the Fe^{3+} reaction during EF, forming complex degradation compounds that are harder

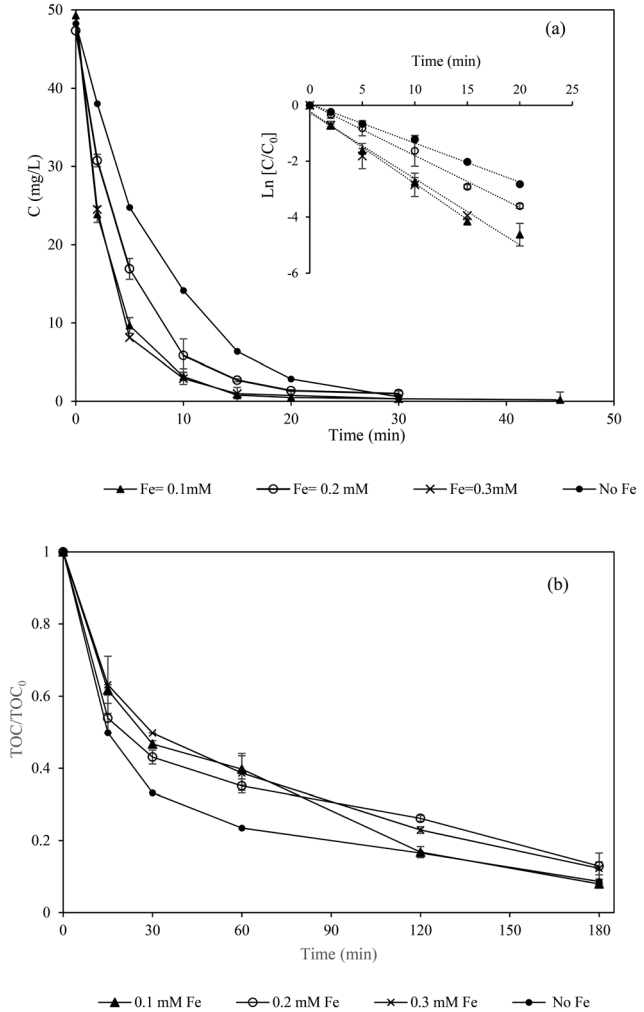

Fig. 4 Effect of iron catalyst Fe^{2+} concentration on MCZ degradation (a) and mineralization (b) during electro-Fenton treatment at a constant current intensity of 150 mA, Na_2SO_4 = 50 mM and pH = 3.

to degrade. In fact, during EF, some carboxylic acids are formed as degradation compounds, and these organic acids can react with Fe^{3+} and generate complexes that are very hard to remove,[12,30] leading to lower mineralization rates during the EF process.

3.4 Effect of the water matrix

The effect of the water matrix on the removal of MCZ was assessed by performing EF in both PW and WWE spiked with 50 mg L^{-1} MCZ. This simulates the application of EF as a tertiary treatment after the biological treatment of (municipal) wastewater. The results in Fig. 5a show the total removal of MCZ in both water matrices. The removal kinetics in the WWE are approximately twice as high as those in the PW, with first-order removal rates of 0.364 min and 0.186 min^{-1}, respectively. The mineralization rate, on the other hand, is similar in the PW and WWE. A similar trend was observed by[33] and[32] for the degradation of a mixture of diclofenac, ibuprofen, and naproxen and the removal of

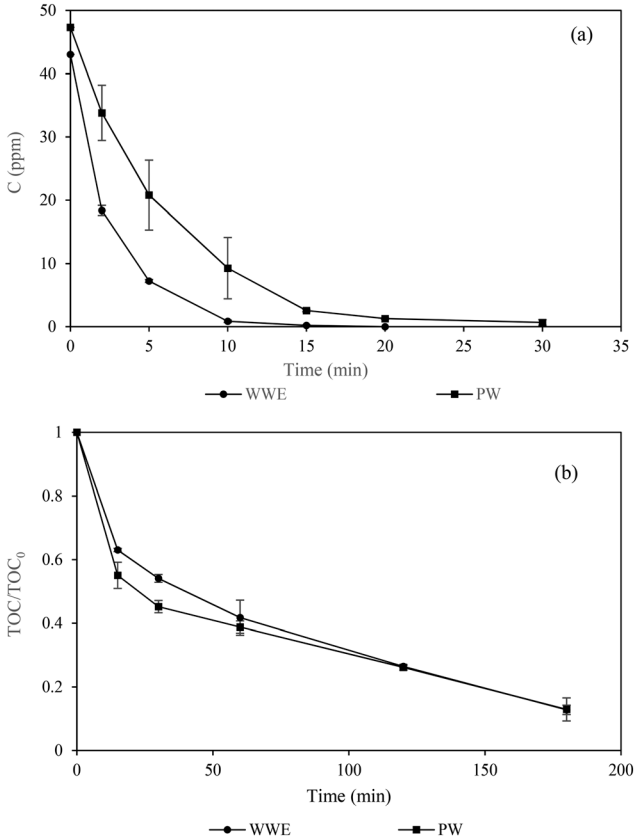

Fig. 5 Effect of water matrix: pure water (PW) and wastewater effluent (WWE) on miconazole (MCZ) degradation (a) and mineralization (b) during electro-Fenton treatment at a constant current intensity of 150 mA, Na_2SO_4 = 50 mM and pH = 3.

caffeine, respectively, *via* the EF process. A possible reason is that the oxidation performance was better in the WWE due to the presence of other ion metals that can contribute to the generation of HO· *via* Fenton-like reactions.[32,34,35] In fact, ICP analysis of the WWE used in this study revealed the presence of various metals and ion metals, as shown in Table 2.

The equations (eqn (12)–(14)) below show examples of Fenton-like reactions that might take place during EF treatment in the presence of different metals.

Table 2 List of elements detected in the wastewater effluents using ICP-MS and their concentrations

Element	Concentration (mg L^{-1})
Al	<0.05
Cd	<0.0002
Cr	<0.004
Fe	0.32
Co	0.0009
Cu	<0.004
Pb	<0.005
Mn	0.17
Ni	<0.01
Ag	<0.005

$$Cu^{+} + H_2O_2 \rightarrow Cu^{2+} + HO\cdot + HO^{-} \quad (12)$$

$$Co^{2+} + H_2O_2 + H^{+} \rightarrow Co^{3+} + HO\cdot + H_2O \quad (13)$$

$$Mn^{2+} + H_2O_2 + H^{+} \rightarrow Mn^{3+} + HO\cdot + H_2O \quad (14)$$

Moreover,[35] showed that removal rates can vary with the type of catalyst metal used during electro-Fenton and Fenton-like treatments. When Ag^{+}, Fe^{2+}, Co^{2+}, and Cu^{2+} ion catalysts were used for the oxidation of metomyl, the order of the kinetics rates was $Fe^{2+} > Co^{2+} > Cu^{2+} > Ag^{+}$.[35]

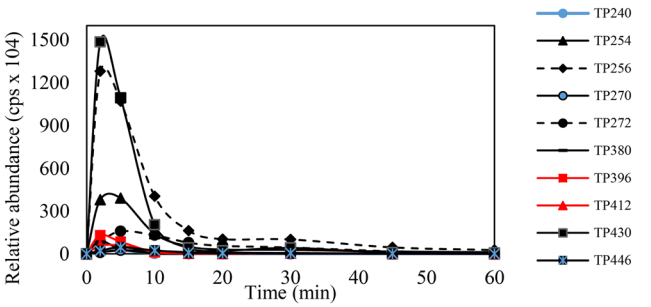

Fig. 7 Time course of formed intermediate compounds during EF treatment of 50 mg L^{-1} MCZ at constant current intensity of 150 mA Fe^{2+} = 0.2 mM Na_2SO_4 = 50 mM.

3.5 Miconazole transformation pathways

Several transformation products (TPs) formed during the EF process were tentatively identified by UHPLC-QTOF-MS. The proposed structures and transformation pathways are presented in Fig. 6. Overall, ten TPs were tentatively identified. Accurate quantification of these TPs was not feasible due to the lack of commercially available standards. Therefore, the evolution of their concentrations as a function of relative abundance and oxidation time is given in Fig. 7. The most common transformations were (i) hydroxylation of the aromatic rings, (ii) dehalogenation and (iii) C–O oxidative cleavage. These transformation mechanisms have previously been suggested by,[36] where the removal of miconazole from wastewater using anodic oxidation was studied. The generation of highly reactive hydroxyl radicals promoted the attack of HO· on the aromatic moieties, which resulted in a mixture of isomers given that the –OH position is undefined. Hence, the consecutive hydroxylation of the aromatic ring produced TP430 (incorporation of one hydroxyl group) and TP446 (incorporation of two hydroxyl groups) while increasing the O:C ratio. The loss of a chlorine atom *via* dehalogenation generated TP380, and the consecutive attack of hydroxyl radicals resulted in the incorporation of 1- or 2-OH moieties to form TP396 and TP412, respectively. Intermediate TP256 was generated from C–O cleavage. This intermediate was further transformed *via* (i) the loss of the hydroxyl moiety, resulting in TP240, (ii) an increase in the O:C ratio *via* hydroxyl radicals attack on

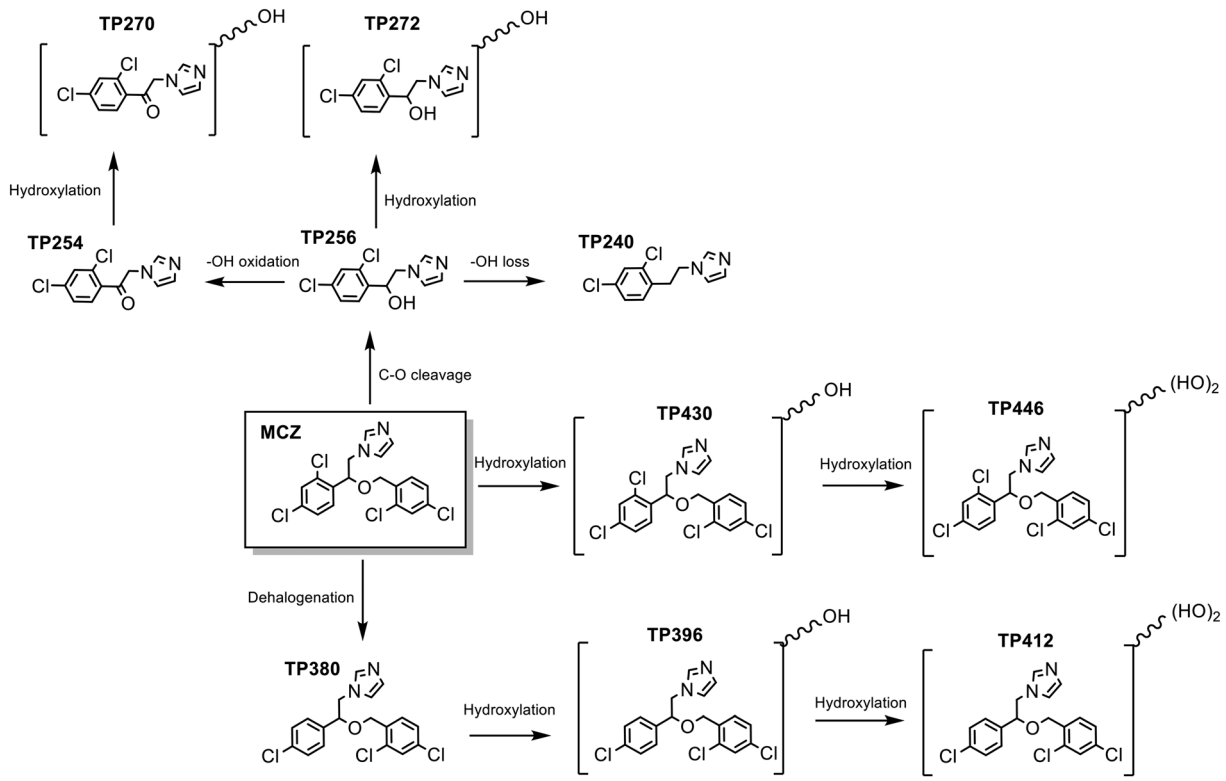

Fig. 6 Miconazole intermediates and degradation pathways during the electro Fenton process of 50 mg L^{-1} MCZ at a constant current intensity of 150 mA Fe^{2+} = 0.2 mM Na_2SO_4 = 50 mM.

the aromatic ring to generate TP272 (addition of one –OH group), (iii) oxidation of the hydroxyl moiety to form a ketone group (TP254). Finally, the aromatic hydroxylation of TP254 generated TP270. Monitoring their time course (Fig. 7) during the EF process revealed their complete elimination after 60 min of reaction time. In contrast with[36] findings, it was found that TPs were recalcitrant toward anodic oxidation, and the EF process showed superior performance in removing these intermediates from wastewater, highlighting the importance of indirect oxidation (*via* the Fenton reaction) within the aqueous medium for the degradation and mineralization of organic compounds.

4. Conclusions

Both EF and AO processes using the BDD anode and carbon felt cathode led to the total removal of miconazole from water. A mineralization efficiency ranging from 80% to 93% after 3 h was achieved, except for the lowest current intensity (50 mA), where a longer electrolysis time (1 h) was required to fully remove MCZ. Faster mineralization rates were observed for AO than for EF, most likely due to the formation of iron complexes in the latter. However, the final removal efficiency was slightly higher when EF with a Fe^{2+} concentration of 0.1 mM was used (92%) compared to AO (88%). Considering the mineralization current efficiency, a specific energy consumption of 150 mA was selected as the most convenient current for MZC removal and mineralization. Low concentrations of Fe^{2+} catalyst allowed the production of homogeneous HO·, improving the efficiency of the process and minimizing parasitic reactions. Crucially, the examination of intermediates through sophisticated methods such as ultra-high-performance liquid chromatography coupled with high-resolution mass spectrometry (UHPLC-HRMS) revealed the presence of ten aromatic oxidation intermediates, offering a valuable understanding of the degradation process. In summary, these results highlight the effectiveness and promise of the electro-Fenton technique as a resilient strategy for eliminating miconazole from water, thus fostering progress in water treatment methodologies and environmental remediation efforts.

Data availability

The data supporting this article will be made available upon request.

Author contributions

Nadia Gadi: writing – original draft-conceptualization-methodology-validation-formal analysis-investigation-visualization-writing – review & editing. Allisson Barros de Souza: resources writing – methodology-formal analysis. Nadine C. Boelee, Deirdre Cabooter, and Raf Dewil: conceptualization; funding acquisition, supervision, writing – review & editing.

Conflicts of interest

The authors declare no competing interests.

Acknowledgements

This research work received funding from the European Union's EU Framework Program for Research and Innovation Horizon 2020 under Grant Agreement No 861369 (MSCA-ETN InnovEOX).

References

1 R. Farooq and Z. Ahmad, *Physico-Chemical Wastewater Treatment and Resource Recovery*, 2017, Available from: **https://www.intechopen.com/books/6050**.
2 T. L. Zearley and R. S. Summers, Removal of Trace Organic Micropollutants by Drinking Water Biological Filters, *Environ. Sci. Technol.*, 2012, **46**(17), 9412–9419.
3 A. Chavoshani, M. Hashemi, M. Mehdi Amin and S. C. Ameta, Pharmaceuticals as emerging micropollutants in aquatic environments, in *Micropollutants and Challenges*, Elsevier, 2020, pp. 35–90, Available from: **https://linkinghub.elsevier.com/retrieve/pii/B9780128186121000027**.
4 J. Rogowska, M. Cieszynska-Semenowicz, W. Ratajczyk and L. Wolska, Micropollutants in treated wastewater, *Ambio*, 2019, **49**(2), 487–503.
5 X. Peng, Q. Huang, K. Zhang, Y. Yu, Z. Wang and C. Wang, Distribution, behavior and fate of azole antifungals during mechanical, biological, and chemical treatments in sewage treatment plants in China, *Sci. Total Environ.*, 2012, **426**, 311–317.
6 European Commission adopts revised Surface Water Watch List. Water Europe, 2020, Available from: **https://watereurope.eu/european-commission-adopts-revised-surface-water-watch-list/**.
7 T. Y. Hargrove, L. Friggeri, Z. Wawrzak, A. Qi, W. J. Hoekstra and R. J. Schotzinger, *et al.* Structural analyses of Candida albicans sterol 14α-demethylase complexed with azole drugs address the molecular basis of azole-mediated inhibition of fungal sterol biosynthesis, *J. Biol. Chem.*, 2017, **292**(16), 6728–6743.
8 R. M. Shah, D. S. Eldridge, E. A. Palombo and I. H. Harding, Microwave-assisted microemulsion technique for production of miconazole nitrate- and econazole nitrate-loaded solid lipid nanoparticles, *Eur. J. Pharm. Biopharm.*, 2017, **117**, 141–150.
9 K. M. Nair, V. Kumaravel and S. C. Pillai, Carbonaceous cathode materials for electro-Fenton technology: Mechanism, kinetics, recent advances, opportunities and challenges, *Chemosphere*, 2021, **269**, 129325.
10 M. A. Oturan, Outstanding performances of the BDD film anode in electro-Fenton process: Applications and comparative performance, *Curr. Opin. Solid State Mater. Sci.*, 2021, **25**(3), 100925.

11 K. Całus-Makowska, J. Dziubińska, A. Grosser and A. Grobelak, Application of the Fenton and photo-Fenton processes in pharmaceutical removal: New perspectives in environmental protection, *Desalin. Water Treat.*, 2025, **321**, 100949.
12 S. Garcia-Segura, Á. S. Lima, E. B. Cavalcanti and E. Brillas, Anodic oxidation, electro-Fenton and photoelectro-Fenton degradations of pyridinium- and imidazolium-based ionic liquids in waters using a BDD/air-diffusion cell, *Electrochim. Acta*, 2016, **198**, 268–279.
13 E. Mousset, N. Oturan and M. A. Oturan, An unprecedented route of OH radical reactivity evidenced by an electrocatalytical process: Ipso-substitution with perhalogenocarbon compounds, *Appl. Catal., B*, 2018, **226**, 135–146.
14 R. Davarnejad and M. Sabzehei, Sodium diclofenac removal from a pharmaceutical wastewater by electro-Fenton process, *Sep. Sci. Technol.*, 2019, **54**(14), 2294–2303.
15 M. Zhou, L. Zhou, L. Liang, F. Yu and W. Yang, Cathode Modification to Improve Electro-Fenton Performance, in *Electro-Fenton Process: New Trends and Scale-Up*, ed. M. Zhou, M. A. Oturan and I. Sirés, The Handbook of Environmental Chemistry, Springer, Singapore, 2018, pp. 175–203, DOI: **10.1007/698_2017_58**.
16 F. Deng, H. Olvera-Vargas, M. Zhou, S. Qiu, I. Sirés and E. Brillas, Critical Review on the Mechanisms of Fe2+ Regeneration in the Electro-Fenton Process: Fundamentals and Boosting Strategies, *Chem. Rev.*, 2023, **123**(8), 4635–4662.
17 A. A. Alvarez-Gallegos and S. Silva-Martínez, Modeling of Electro-Fenton Process, in *Electro-Fenton Process: New Trends and Scale-Up*, ed. M. Zhou, M. A. Oturan and I. Sirés, The Handbook of Environmental Chemistry, Springer, Singapore, 2018, pp. 287–312, DOI: **10.1007/698_2017_73**.
18 N. A. Bury, K. A. Mumford and G. W. Stevens, The electro-Fenton regeneration of Granular Activated Carbons: Degradation of organic contaminants and the relationship to the carbon surface, *J. Hazard. Mater.*, 2021, **416**, 125792.
19 P. V. Nidheesh and R. Gandhimathi, Trends in electro-Fenton process for water and wastewater treatment: An overview, *Desalination*, 2012, **299**, 1–15.
20 I. Sirés and E. Brillas, Electro-Fenton Process: Fundamentals and Reactivity, in *Electro-Fenton Process: New Trends and Scale-Up*, ed. M. Zhou, M. A. Oturan and I. Sirés, The Handbook of Environmental Chemistry, Springer, Singapore, 2018, pp. 1–28, DOI: **10.1007/698_2017_40**.
21 C. Annabi, F. Fourcade, I. Soutrel, F. Geneste, D. Floner and N. Bellakhal, *et al.*, Degradation of enoxacin antibiotic by the electro-Fenton process: Optimization, biodegradability improvement and degradation mechanism, *J. Environ. Manage.*, 2016, **165**, 96–105.
22 M. A. Oturan and J. J. Aaron, Advanced Oxidation Processes in Water/Wastewater Treatment: Principles and Applications, A Review, *Crit. Rev. Environ. Sci. Technol.*, 2014, **44**(23), 2577–2641.
23 J. Feng, Electrochemical oxidation of sulfamethoxazole by nitrogen-doped carbon nanosheets composite PbO2 electrode: Kinetics and mechanism – ScienceDirect, 2022, Available from: **https://www.sciencedirect.com/science/article/abs/pii/S0045653521020828?fr=RR-2&ref=pdf_download&rr=7188b824bf29b8e5**.
24 I. Sirés and E. Brillas, Remediation of water pollution caused by pharmaceutical residues based on electrochemical separation and degradation technologies: A review, *Environ. Int.*, 2012, **40**, 212–229.
25 R. V. McQuillan, G. W. Stevens and K. A. Mumford, The electrochemical regeneration of granular activated carbons: A review, *J. Hazard. Mater.*, 2018, **355**, 34–49.
26 O. Ganzenko, C. Trellu, N. Oturan, D. Huguenot, Y. Péchaud and E. D. van Hullebusch, *et al.* Electro-Fenton treatment of a complex pharmaceutical mixture: Mineralization efficiency and biodegradability enhancement, *Chemosphere*, 2020, **253**, 126659.
27 E. Bocos, N. Oturan, M. Á. Sanromán and M. A. Oturan, Elimination of radiocontrast agent Diatrizoic acid from water by electrochemical advanced oxidation: Kinetics study, mechanism and mineralization pathway, *J. Electroanal. Chem.*, 2016, **772**, 1–8.
28 M. Panizza and G. Cerisola, Direct And Mediated Anodic Oxidation of Organic Pollutants, *Chem. Rev.*, 2009, **109**(12), 6541–6569.
29 D. Martínez-Pachón, Treatment of two sartan antihypertensives in water by photo-electro-Fenton using BDD anodes: Degradation kinetics, theoretical analyses, primary transformations and matrix effects, *Chemosphere*, 2021, **270**, 129491.
30 Y. Y. Chu, Y. Qian, W. J. Wang and X. L. Deng, A dual-cathode electro-Fenton oxidation coupled with anodic oxidation system used for 4-nitrophenol degradation, *J. Hazard. Mater.*, 2012, **199–200**, 179–185.
31 N. Oturan, S. O. Ganiyu, S. Raffy and M. A. Oturan, Sub-stoichiometric titanium oxide as a new anode material for electro-Fenton process: Application to electrocatalytic destruction of antibiotic amoxicillin, *Appl. Catal., B*, 2017, **217**, 214–223.
32 N. Gadi, N. C. Boelee and R. Dewil, The Electro-Fenton Process for Caffeine Removal from Water and Granular Activated Carbon Regeneration, *Sustainability*, 2022, **14**(21), 14313.
33 M. Villanueva-Rodríguez, R. Bello-Mendoza, A. Hernández-Ramírez and E. J. Ruiz-Ruiz, Degradation of anti-inflammatory drugs in municipal wastewater by heterogeneous photocatalysis and electro-Fenton process, *Environ. Technol.*, 2019, **40**(18), 2436–2445.
34 Y. Xue, Electrochemical detoxification and recovery of spent SCR catalyst by in-situ generated reactive oxygen species in alkaline media – ScienceDirect, 2017, Available from: **https://www.sciencedirect.com/science/article/abs/pii/S1385894717308641?fr=RR-2&ref=pdf_download&rr=7964c32e1e63b90e**.
35 N. Oturan, M. Zhou and M. A. Oturan, Metomyl Degradation by Electro-Fenton and Electro-Fenton-Like Processes: A Kinetics Study of the Effect of the Nature and Concentration

of Some Transition Metal Ions As Catalyst, *J. Phys. Chem. A*, 2010, **114**(39), 10605–10611.

36 A. B. De Souza, J. Mielcke, I. Ali, R. Dewil, T. Van De Goor and D. Cabooter, Removal of miconazole from water by O3, UV/H2O2 and electrochemical advanced oxidation: Real-time process monitoring and degradation pathway elucidation, *J. Environ. Chem. Eng.*, 2023, **11**(3), 109993.